

Experimental evidence for an intermediate phase in the multiferroic YMnO₃

Gwilherm Nénert¹, Michael Pollet², Sylvain Mariné³, Yang Ren⁴, Auke Meetsma¹ and Thomas T. M. Palstra¹

¹*Solid State Chemistry Laboratory, Materials Science Centre,
University of Groningen, Nijenborg 4, 9747 AG Groningen, The Netherlands*

²*ICMCM - CNRS Physico-Chimie des Oxydes Conducteurs,
87 Avenue du Doctor Schweitzer 33608 Pessac Cedex France*

³*CRISMAT - ENSI Bd Maréchal Juin - 14050 Caen Cedex 4 France and*

⁴*Experimental Facilities Division, Advanced Photon Source,
Argonne National Laboratory, Argonne, Illinois 60439, USA*

We have carried out high temperature synchrotron x-ray experiments, differential scanning calorimetry and thermomechanical analysis on a single-crystal of YMnO₃ grown by the Floating Zone Technique. These experiments show two anomalies at about 1100K and 1350K demonstrating the existence of an intermediate phase between the ferroelectric P6₃cm structure and the high temperature centrosymmetric phase with P6₃/mmc symmetry. This work identifies for the first time the different high temperature phase transitions in YMnO₃.

PACS numbers: PACS numbers: 61.10.Nz,77.80.Bh

I. INTRODUCTION

In typical ferroelectrics creation of the electric dipole moment involves charge transfer between the empty d shell metal ions and the occupied 2p orbitals of the oxygen. This mechanism of ferroelectricity precludes magnetic moments and magnetic order. YMnO₃ is part of a class of materials that exhibit both electric and magnetic orders, called multiferroics. The coexistence of ferroelectricity and magnetic order allows the manipulation of electric and magnetic moments by magnetic and electric fields, respectively¹. In the multiferroics, the charge transfer from the 2p orbitals towards the transition metal ion is not relevant due to the partially filled nature of the d-shell. Indeed, in YMnO₃ the Mn-ion is in the barycenter of its oxygen coordination. However, this charge transfer is allowed towards the empty d shell of the rare-earth². This charge transfer creates two dipoles of opposite sign resulting in a ferroelectric state of YMnO₃. Recent ab-initio calculations indicate that the ferroelectric state involves no charge-transfer, but is related to the tilting of the MnO₅ polyhedra. However, there is no clear structural information about this transition to clarify the origin of the ferroelectric state in these materials.

While a lot of effort is put in the search and design of new multiferroics, the nature of the mechanism of ferroelectricity and thus the nature of the coupling between the different degrees of freedom is still not well understood. We can distinguish two classes of magnetoferroelectrics: T_N (Néel temperature) $>$ T_{FE} (critical temperature for ferroelectricity) and $T_N <$ T_{FE} . For the first class, with compounds like RMn₂O₅ and o-RMnO₃ (orthorhombic), the mechanism of ferroelectricity can be understood phenomenologically by a term in the free energy of the type $PM\partial M$ where P is the polarization and M the magnetization^{3,4}. The coexistence and strong coupling between ferroelectricity and incommensurate magnetism in o-RMnO₃ is related to Dzyaloshinskii-Moriya interactions⁵. For the second class, which includes h-

RMnO₃ (hexagonal), the origin of ferroelectricity is not well understood since the Mn off centering is not responsible for the ferroelectricity². Moreover, the h-RMnO₃ is particularly interesting due to the high polarization at room temperature ($P_S \sim 5.5 \mu\text{C}/\text{cm}^2$). The h-RMnO₃ exhibit $T_{FE} \sim 1000$ K and $T_N \sim 100$ K. Recent studies of h-RMnO₃ show that the ferroelectric and antiferromagnetic order parameters are coupled^{6,7,8,9}.

The research history on YMnO₃, reports mention several transition temperatures above room temperature. To clarify the often conflicting transition temperatures, we will present a brief historical review of the different studies on YMnO₃. Next, we will report the first crystal structure of Bi-free single-crystal and make a comparative study between flux grown and floating zone grown single-crystal. Then, we will show that in the high temperature regime, there are two distinct phase transitions. We present evidence first from disappearance of several Bragg reflections in x-ray diffraction, second from anomalies in the differential scanning analysis, and third from the thermomechanical response.

II. HISTORICAL PERSPECTIVE

Bertaut and coworkers¹⁰ were the first to discover ferroelectricity in several compounds of the h-RMnO₃ family (R = Er, Lu and Y). They measured the P-E hysteresis and polarization on single-crystal grown from Bi₂O₃ flux. The same year, Bokov *et al.* confirmed the observations of Bertaut *et al.* and measured the magnetic properties down to 77K of single-crystal of Y and Yb grown also from Bi₂O₃ flux. They were the first to mention the antiferromagnetic order of these compounds¹¹. They reported a saturated polarization at room temperature of $5.5 \mu\text{C}/\text{cm}^2$. One year later, Smolenskii *et al.* confirmed the ferroelectricity and the antiferromagnetic ordering of the Mn³⁺ spins of YMnO₃ and YbMnO₃¹². They report also that no ferroelectric transition could be

observed below 823K. Also they grew the single-crystals from a Bi_2O_3 flux.

The first experimental observations of the ferroelectric transition in YMnO_3 was the work of Ismailzade and Kizhaev¹³. They reported the pyroelectric current of single-crystals of YMnO_3 and YbMnO_3 . They observed a peak in these measurements at about 933K and 973-998K respectively. These observations were confirmed by anomalies in the cell parameters at about 933K for YMnO_3 and at about 998K for YbMnO_3 . However, the temperature dependence of the cell parameters is different from all later reports. In addition, they observed anomalies in the thermal expansion at about 498K and 623K for YMnO_3 and YbMnO_3 respectively. Also these observations were never reproduced in later reports. The single-crystals were also grown from Bi_2O_3 flux. They were the first to propose the $\text{P6}_3/\text{mcm}$ symmetry for the phase above the ferroelectric transition. However they did not provide any evidence. Soon afterwards, Peuzin *et al.* reported on YMnO_3 single-crystal a dielectric constant of 20¹⁴. The dielectric constants and $\tan(\delta)$ were independent of the frequency between 50Hz and 50MHz for their crystals. Moreover they found that the resistivity of YMnO_3 followed an Arrhenius law with an activation energy of 1.4eV between room temperature and 923K. Coeure *et al.* have reported a ferroelectric transition at about 913K in YMnO_3 confirming the results of Ismailzade and Kizhaev¹⁵. Much later, Lukaszewicz and Karut-Kalicińska investigated YMnO_3 by high temperature single-crystal x-ray. They reported in the region 893-953K small anomalies in the lattice constants that they ascribed to the ferroelectric phase transition¹⁶. In addition, they observed for $T > 1273\text{K}$, a change in symmetry with the space-group $\text{P6}_3/\text{mmc}$. However they failed to refine their data below 1273K with the $\text{P6}_3/\text{mcm}$ symmetry proposed earlier by Ismailzade. We notice from this literature review that there have been two different transition temperatures. However they were never observed both in one single experiment. Moreover it was consistently reported that the ferroelectric transition of YMnO_3 is about 933K, in contrast with the claim by Abrahams¹⁷. However, the symmetry of the intermediate phase (IP) has not been established.

In recent years, two structure studies have been carried out in the high temperature regime either by synchrotron or neutron diffraction on h- RMnO_3 powder^{18,19}. Both experiments failed to observe any structural phase transitions even though they measured up 1000K for R = Y (synchrotron), up to 1300K for Lu, 1100K for Yb and 1400K for Tm (neutron). Lonkai *et al.* realized the necessity for two high temperature phase transitions, based on symmetry arguments. Therefore, they proposed an anti-ferroelectric IP having the same symmetry as the room temperature phase. We think that the absence of observations of phase transitions in these two recent studies, contradicting with older results caused confusion regarding the transition temperatures. Furthermore the succession of states was not always incorporated in investiga-

tions of the origin of the ferroelectric state^{2,20}. The aim of this paper is to proof experimentally the existence of the IP in YMnO_3 and to show that our data are in full agreement with previous observations.

We provide experimental proof for the existence of an IP using Differential Scanning Analysis and Thermomechanical Analysis. These results fully support the results of the early investigations on YMnO_3 . Our work contradicts previous analyses^{2,19}. Moreover, we explain the differences in the critical temperatures between our results and earlier reports on Bi-free grown single-crystal.

III. EXPERIMENTAL TECHNIQUES

YMnO_3 powder was synthesized by reacting stoichiometric amounts of Y_2O_3 (4N) and MnO_2 (3N metal basis) in nitrogen atmosphere at 1200°C for 10h. The powder was reground and resintered once under the same conditions to improve crystallinity. A single crystal was grown from the powder in air by the Floating Zone technique using a four mirror furnace. The crystallinity of the crystal was checked by Laue diffraction. The high quality of the crystal is further evidenced by narrow diffraction peaks ($\Delta 2\theta \sim 0.012^\circ$ at RT).

High temperature diffraction experiments were performed on beamline BESSRC-11-ID-C at the Advanced Photon Source using a wavelength of 10.772 pm. The sample was heated in air using a four mirror furnace. We note that experiments by other groups were performed in vacuum, which may result in off-stoichiometry or even partial decomposition of the sample. The data were analyzed using the FIT2D program²¹ to convert our image plate data to a 2D powder pattern, and then by the GSAS software package²². A black colored irregular crystal extracted from the grown boule with the approximate dimensions of 0.14×0.12×0.04 mm was mounted on a Bruker SMART APEX CCD diffractometer (Platform with full three-circle goniometer). The diffractometer was equipped with a 4K CCD detector set 60.0 mm from the crystal. Intensity measurements were performed using graphite monochromatic Mo-K_α radiation. SMART was used for preliminary determination of the unit cell constants and data collection control. The intensities of reflections of a hemisphere were collected by a combination of 3 sets of exposures (frames). Each set had a different ϕ angle for the crystal and each exposure covered a range of 0.3° in ω . A total of 3600 frames were collected with an exposure time of 10.0 seconds per frame. Data integration and global cell refinement was performed with the program SAINT. The final unit cell was obtained from the xyz centroids of 1743 reflections after integration. Intensity data were corrected for Lorentz and polarization effects, scale variation, for decay and absorption: a multi-scan absorption correction was applied, based on the intensities of symmetry-related reflections measured at different angular settings (SADABS)²³, and reduced to F_{obs}^2 . The program suite SHELXTL was used for space

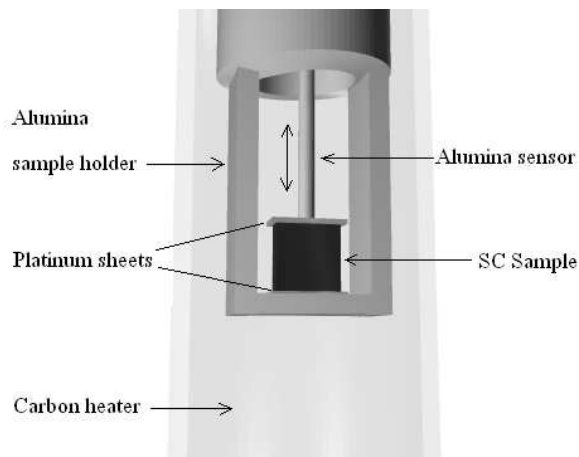


FIG. 1: Set-up used to measure the thermomechanical behavior of our single-crystal.

group determination assuming an inversion twin²⁴.

The differential scanning analysis was carried out in a flow of nitrogen using TA Instruments - SDT 2960 apparatus. The temperature ramp was 5K/min. We have used a crushed single-crystal for this experiment in a platinum pan.

The dilatometric measurements were carried out in static air using a SETARAM TMA92 dilatometer. The temperature ramps were 1 K/min with a dwell at 1473 K for half an hour. A load of 10 g was applied to optimize the signal to noise ratio. The choice of this slight load is based on several trial runs. The single-crystal sample was protected from the alumina parts (see figure 1) using platinum sheets. All the measurements were corrected with the blank signal (alumina + platinum).

IV. EXPERIMENTAL RESULTS

We have solved the structure of a single-crystal grown by the floating zone technique. The atomic coordinates and the isotropic thermal parameters are presented in table 1. This structure is very similar to the previous reported single-crystal structures of YMnO_3 . However there is one main difference which is the value of the c axis; compared with the structures of the single-crystals grown from Bi_2O_3 flux (Cf. table 2). We discuss in the next section the origin of this difference and its consequence for the ferroelectric transition temperature.

In Figure 2, we show the temperature dependence of the thermomechanical response of a single-crystal of YMnO_3 . We observe clearly two anomalies while heating. The first anomaly, denoted T_{C1} , appears at about 1125K and the second anomaly appears at $T_{C2} \sim 1275\text{K}$. These anomalies are confirmed in our DSC experiment, shown in figure 3, where we notice a small anomaly at about 1100K for T_{C1} and at $\sim 1350\text{K}$ for T_{C2} . This difference in the critical temperature T_{C2} can be explained

Atoms	x	y	z	U_{eq} (\AA^2)
Y_1	0.00000	0.00000	0.2711(2)	0.0056(5)
Y_2	-0.66667	-0.33333	0.23038(-)	0.0060(3)
Mn	-0.3328(5)	-0.3328(5)	-0.0024(2)	0.0059(5)
O_1	-0.3025(13)	-0.3025(13)	0.1611(11)	0.010(2)
O_2	0.3530(12)	0.3530(12)	0.3352(9)	0.005(2)
O_3	0.00000	0.00000	0.473(2)	0.008(3)
O_4	-0.66667	-0.33333	0.0150(14)	0.010(3)

$wR(F^2) = 8.45\%$ and $R(F) = 3.43\%$

TABLE I: Atomic coordinates of our free Bi single-crystal with cell parameters $a = 6.1469(6)\text{\AA}$ and $c = 11.437(1)\text{\AA}$. In brackets, we indicate the relative error.

Reference	a (\AA)	c (\AA)
Ref. 16	6.145	11.42
Ref. 25	6.1387	11.4071
Ref. 13	6.125	11.41
Our data	6.1469(6)	11.437(1)

TABLE II: Comparison between single-crystal grown from Bi_2O_3 flux and our data.

by the strong first order character of the transition.

In Figure 4, we show the temperature dependence of the square root of the integrated intensity of a selected reflection (102). The disappearance of this reflection while the reflection (113) remains above T_{C2} signals the tripling of the unit-cell at around 1275K. Among the possible high temperature phases for YMnO_3 , the tripling of the unit-cell at T_{C2} can be explained only by a change of symmetry towards the $P6_3/mmc$ symmetry.

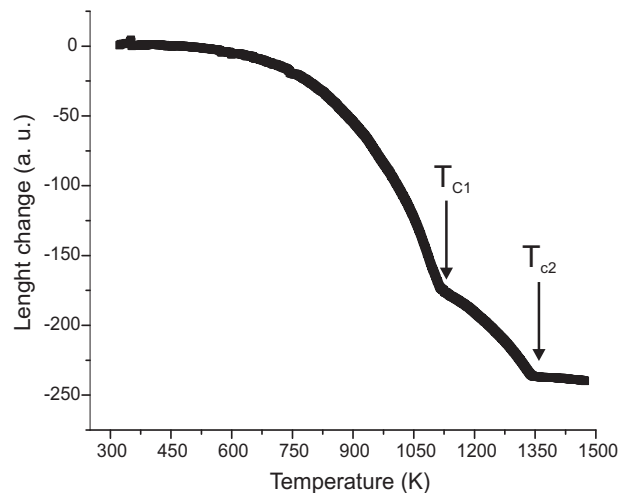


FIG. 2: Thermomechanical response of a single-crystal of YMnO_3 . The arrows indicate the ferroelectric transition temperature T_{C1} and the tripling of the unit cell T_{C2} .

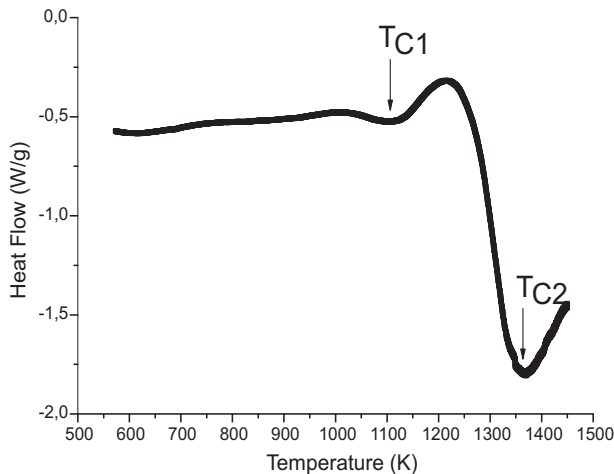


FIG. 3: Differential Scanning Analysis of a crushed single-crystal of YMnO_3 . The measurement has been carried out in N_2 atmosphere with a rate of $5\text{K}/\text{min}$. The arrows indicate the ferroelectric transition temperature T_{C1} and the tripling of the unit cell T_{C2} .

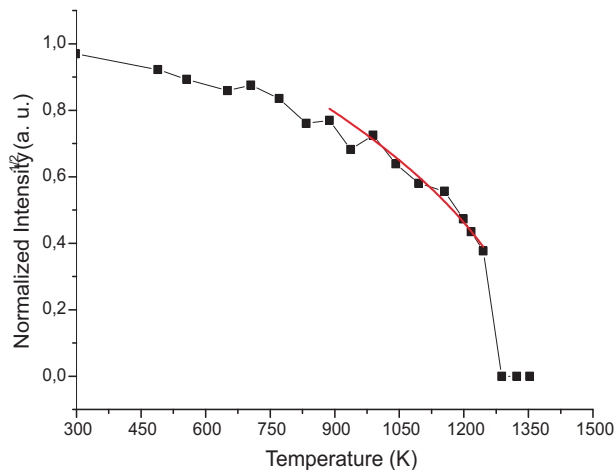


FIG. 4: (Color Online) Square root of the integrated intensity of the reflection (102) versus temperature. In red, square root dependence near T_{C2} of the square root of the integrated intensity

V. DISCUSSION

This manuscript reports for the first time two consecutive phase transitions in YMnO_3 . This is evidenced by x-ray diffraction, two anomalies in the thermomechanical response and in the DSC results. In the DSC experiment, we notice a small anomaly at T_{C1} and a larger one at T_{C2} . We relate the different thermodynamic response to the changes in crystal symmetry as dictated by group theory. Thermodynamics relate discontinuous first order derivatives of the Gibbs free energy with the enthalpy (latent heat) ΔH . The area of a peak in a DSC scan (whether endothermic or exothermic) is related to the enthalpy change (ΔH)²⁶. In our DSC signal, we can

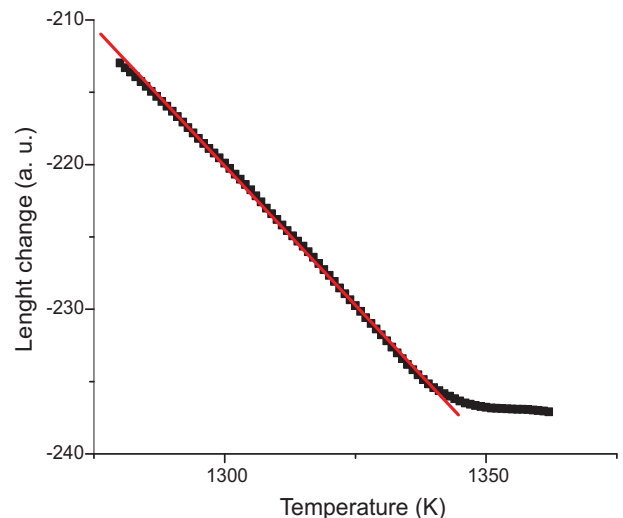


FIG. 5: (Color Online) Linear fit of the thermomechanical response near T_{C1} .

notice a large peak at about 1350K which proves the 1^{st} order nature of the transition. This is in agreement with our symmetry analysis (presented elsewhere)²⁷ in the hypothesis of going from $P6_3/mcm$ (IP) to $P6_3/mmc$ (HT). This transition corresponds to the tripling of the unit cell going towards the centrosymmetric space-group $P6_3/mmc$. This transition is characterized by a primary order parameter which behaves as $(T-T_{C2})^{1/2}$. In contrast with the integrated intensity, the secondary order parameter (TMA experiment) behaves as $(T-T_{C2})$ as presented in figure 5. We explain the difference in T_{C2} between our DSC/TMA experiments and our synchrotron data the first order nature of the transition.

Moreover, we observe a small anomaly at about 1100K which we relate to the ferroelectric transition. The DSC anomaly is small compared to the peak near 1350K . We interpret the nature of the ferroelectric transition as being second order or weak first order.

As we already noticed, the c cell parameter for single-crystal grown from a Bi_2O_3 flux is systematically smaller than for crystal grown by the floating zone technique. There are two possibilities to explain this difference: either a significant amount of Bi incorporated in the structure or/and a significant amount of vacancies in the crystal structure. We expect that if Bi is incorporated into the structure, it will preferentially go on the yttrium site. For this purpose, we compare the Shannon radius of Bi and Y: $r(\text{Bi}^{3+}) = 1.24\text{\AA}$ (derived from the average between 6-fold coordination and 8-fold coordination of Bi) and $r(\text{Y}^{3+}) = 1.1\text{\AA}$. We conclude that since the Bi is bigger than Y, we expect an enlargement of the cell parameters. Moreover, we have carried out a refinement of the occupation on both site of Y using the data of van Aken *et al.* and our data. We did not find any evidence for a replacing of Y by Bi in the case of the data of van Aken *et al.* Thus, we can disregard the incorporation of Bi inside the

structure. Obviously the crystal growth in the Floating Zone techniques occurs at considerably higher temperature than in the Bi-flux. According to Abrahams²⁸, we have (in Kelvin):

$$T_{FE} = (\kappa/2k)(\Delta z)^2 \quad (1)$$

where κ is a force constant, k is Boltzmann's constant and Δz is the largest displacement along the polar c axis in Å. The ratio $\kappa/2k$ has been estimated to be $2.00(9) \times 10^4 \text{ KÅ}^{-2}$. According to equation 1, the only ways to decrease T_{FE} are to decrease the force constant, the displacement of the rare earth z and/or the c axis parameter. It is obvious that defects can be responsible for such changes. For instance, an excess in yttrium ($\text{YMn}_{1-x}\text{O}_{3-3/2x}$) would certainly both decrease the c parameter (consistent with the observations) and lower κ . In the same way, impurities can lower T_{FE} . It has been checked through the structure refinement of van Aken samples that no Bi was inserted in the structure. However, let's consider, for instance, an experiment made using alumina crucibles instead of platinum and one can easily obtain $\text{YMn}_{1-x}\text{Al}_x\text{O}_3$. Such a substitution would again account for a small decrease in the c parameter. All of these suggestions need to be experimentally checked.

This revisited value of $T_{C1}=T_{FE}$ can explain the main features of the recent experiments by Lonkai et Katsufuji. Both groups used powders whereas all previous results in older literature were performed on single-crystals grown from a Bi-flux. Indeed, both experiments failed to observe any phase transition, except for Tm where Lonkai *et al.* observed incipient behavior, however without reaching the IP. Katsufuji *et al.* have measured until

1000K on YMnO_3 , synthesized in air, while our experiments show a transition at 1100K. For Lu and Yb, Lonkai *et al.* like Katsufuji and coworkers did not measure sufficiently high enough in temperature in order to observe a phase transition. For these smaller rare-earths the ferroelectric transition is expected to be higher than for Y¹⁷.

VI. CONCLUSION

In conclusion, we observed two consecutive high temperature phase transitions in YMnO_3 using synchrotron x-ray data, thermomechanical analysis and DSC. We ascribe these transitions to the ferroelectric transition and a tripling of the unit cell, respectively. We explain the somewhat higher critical temperature for the ferroelectric transition $T_{FE} \sim 1100\text{K}$ of our sample as the result of sample synthesis. The transitions are second (or weakly first order) and first order in nature, respectively, in agreement with our symmetry analysis. However, the symmetry of the intermediate phase remains to be investigated. Further experiments are in progress in order to give a full description of this system.

VII. ACKNOWLEDGEMENT

We thank fruitful discussions with Dr. Beatriz Noheda. One of the author (G. Nénert) acknowledge stimulating discussions with Prof. Harold Stokes. This research is part of the MSC^{plus} program. Use of the Advanced Photon Source was supported by the U. S. Department of Energy Office of Science, Office of Basic Energy Sciences, under contract No-W-37-109-Eg-38.

-
- * Corresponding author: t.t.m.palstra@rug.nl
- ¹ J. Wang *et al.*, Science **299**, 1719(2003); Kimura *et al.*, Nature **426**, 55 (2003) and Hur *et al.*, Nature **429**, 392 (2004)
 - ² B. van Aken *et al.* Nature Materials **3**, 164 - 170 (2004)
 - ³ M. Mostovoy, cond-mat/0510692
 - ⁴ H. Katsura, N. Nagaosa and A. V. Balatsky, Phys. Rev. Lett. **95**, 57205 (2005)
 - ⁵ I. A. Sergienko and E. Dagotto, cond-mat/0508075
 - ⁶ Z. J. Huang *et al.*, Phys. Rev. B **56**, 2623 (1997)
 - ⁷ M. N. Iliev *et al.*, Phys. Rev. B **56**, 2488 (1997)
 - ⁸ M. Fiebig *et al.*, Nature **419**, 818 (2002)
 - ⁹ B. Lorenz, A. P. Litvinchuk, M. M. Gospodinov, and C. W. Chu, Phys. Rev. Lett. **92**, 87204 (2004)
 - ¹⁰ Bertaut *et al.* (1963) (C. R. Acad. Sci. Paris, 256, pp1958-1961)
 - ¹¹ Bokov *et al.* Sov. Phys. Solid State, vol. 5, pp2646-2647,1964
 - ¹² Smolenskii *et al.* (1964) J. Appl. Phys., 35,pp915-918
 - ¹³ I. G. Ismailzade *et al.*, Sov. Phys. Solid State, **70**, 236 (1965)
 - ¹⁴ Jean-Claude Peuzin, C. R. Acad. Sc. Paris, **261**, 2195-2197 (1965)
 - ¹⁵ Coeure *et al.* Proceedings of the International Meeting on Ferroelectricity, **1**, 332 (1966)
 - ¹⁶ K. Lukaszewicz *et al.*, Ferroelectrics **7**, 81-82 (1974)
 - ¹⁷ S. C. Abrahams *et al.*, Acta Cryst.
 - ¹⁸ Katsufuji *et al.*, Phys. Rev. B **66**, 134434 (2002)
 - ¹⁹ T. Lonkai *et al.*, Phys. Rev. B **69**, 134108 (2004)
 - ²⁰ C. J. Fennie and K. M. Rabe, Phys. Rev. B **72**, 100103 (2005)
 - ²¹ FIT2D V10.3, A. P. Hammersly/ESRF 1987-1998.
 - ²² A. C. Larson and R. B. von Dreele, General Structure Analysis System GSAS, Los Alamos National Laboratory Report No. LAUR 86-748, 1994 (unpublished).
 - ²³ Sheldrick, G.M. (2001). SADABS. Version 2. Multi-Scan Absorption Correction Program. University of Gttingen, Germany
 - ²⁴ Bruker (2000). SMART, SAINT, SADABS, XPREP and SHELXTL/NT. Area Detector Control and Integration Software. Smart Apex Software Reference Manuals. Bruker Analytical X-ray Instruments. Inc., Madison, Wisconsin, USA
 - ²⁵ B. van Aken, A. Meetsma and T. T. M. Palstra, Acta Cryst. C (2001) **57**, 230-232
 - ²⁶ Comprehensive Supramolecular Chemistry, vol. 8, Physical methods in Supramolecular Chemistry, Edited by J. Eric

D. Davies and John A. Ripmeester (1996)

Rev. **172**, 551 (1968)

²⁷ G. Nénert *et al.*, in preparation

²⁸ S. C. Abrahams, S. K. Kurtz and P. B. Jamieson, Phys.